ACS central science

Research Article

http://pubs.acs.org/journal/acscii

Catalytic N_2-to-NH_3 Conversion by Fe at Lower Driving Force: A Proposed Role for Metallocene-Mediated PCET

Matthew J. Chalkley,[†] Trevor J. Del Castillo,[†] Benjamin D. Matson,[†] Joseph P. Roddy, and Jonas C. Peters*

Division of Chemistry and Chemical Engineering, California Institute of Technology (Caltech), Pasadena, California 91125, United States

Supporting Information

ABSTRACT: We have recently reported on several Fe catalysts for N_2-to-NH_3 conversion that operate at low temperature (−78 °C) and atmospheric pressure while relying on a very strong reductant (KC_8) and acid ($[H(OEt_2)_2][BAr^F{}_4]$). Here we show that our original catalyst system, $P_3{}^BFe$, achieves both significantly improved efficiency for NH_3 formation (up to 72% for e^- delivery) and a comparatively high turnover number for a synthetic molecular Fe catalyst (84 equiv of NH_3 per Fe site), when employing a significantly weaker combination of reductant ($Cp^*{}_2Co$) and acid ($[Ph_2NH_2][OTf]$ or $[PhNH_3][OTf]$). Relative to the previously reported catalysis, freeze-quench Mössbauer spectroscopy under turnover conditions suggests a change in the rate of key elementary steps; formation of a previously characterized off-path borohydrido−hydrido resting state is also suppressed. Theoretical and experimental studies are presented that highlight the possibility of protonated metallocenes as discrete PCET reagents under the present (and related) catalytic conditions, offering a plausible rationale for the increased efficiency at reduced driving force of this Fe catalyst system.

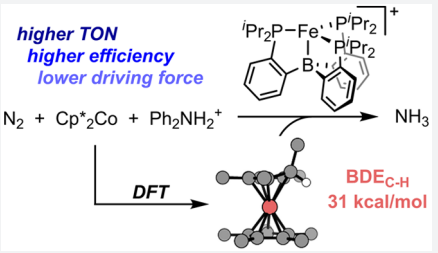

The reduction of N_2 to NH_3 is critical for life and is performed on a massive scale both industrially and biologically.[1] The high stability of the N≡N triple bond necessitates catalysts and high-energy reagents/conditions to achieve the desired transformation.[2] Synthetic studies of catalytic N_2-to-NH_3 conversion by model complexes are of interest to constrain hypotheses concerning the mechanism/s of biological (or industrial) N_2-fixation and to map fundamental catalyst design principles for multielectron reductive transformations.[3,4] Interest in Fe model systems that catalyze N_2-to-NH_3 conversion has grown in part due to the postulate that one or more Fe centers in the FeMo-cofactor of FeMo-nitrogenase may serve as the site of N_2 binding and activation during key bond-breaking and -making steps.[5] Previous examples of synthetic molecular Fe catalysts that mediate N_2-to-NH_3 conversion operate with high driving force, relying on a very strong acid (pK_a ca. 0) and reductant ($E^\circ \leq -3.0$ V vs $Fc^{+/0}$).[6−9] In contrast, several Mo catalysts have been shown to facilitate N_2-to-NH_3 conversion with significantly lower driving force.[10−13] There is thus interest in exploring the viability of Fe-mediated catalytic N_2-to-NH_3 conversion under less forcing conditions from a practical perspective, and to continue assessing these systems as functional models of biological nitrogenases, in which 8 ATP are consumed per NH_3 formed providing a total driving force of 58 kcal/mol.[2]

Herein we demonstrate that catalytic conversion of N_2 to NH_3 by $P_3{}^BFe^+$ ($P_3{}^B$ = tris(*o*-diisopropylphosphinophenyl)-borane) can be achieved with a significantly lower driving force by coupling $Cp^*{}_2Co$ with $[Ph_2NH_2]^+$ or $[PhNH_3]^+$ (Figure 1).

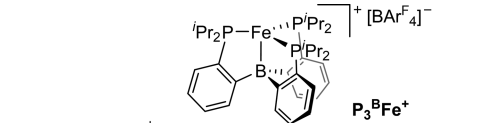

e⁻ (E^0 vs $Fc^{+/0}$)	H^+ (pK_a in THF)	$\Delta\Delta H_f$ (kcal/mol)	% yield NH_3
$Cp^*{}_2Co$ (-1.96 V)	$[PhNH_3][OTf]$ (7.6)	59	38
$Cp^*{}_2Co$ (-1.96 V)	$[Ph_2NH_2][OTf]$ (3.2)	77	72
KC_8 (≤ -3.0 V)	$HBAr^F{}_4$ (≤ 0)	≥ 156	45

Figure 1. Summary of conditions used for catalytic N_2-to-NH_3 conversion by $P_3{}^BFe^+$ highlighting the estimated enthalpic driving force ($\Delta\Delta H_f$).[14−19]

Such conditions additionally afford unusually high selectivity and catalytic turnover for NH_3.[20] Moreover, we note that the use of milder reagents as reductant (E^0; eq 1) and acid (pK_a; eq 1) engenders a higher effective bond dissociation enthalpy ($BDE_{effective}$; eq 1).[15,21] This may in turn afford access to proton-coupled electron transfer (PCET) pathways (e.g., $FeN_2 + H^\bullet \rightarrow FeN_2H$) in addition to electron transfer (ET)/proton transfer (PT) pathways, thus enhancing overall catalytic

Received: January 9, 2017
Published: February 14, 2017

DOI: 10.1021/acscentsci.7b00014
ACS Cent. Sci. 2017, 3, 217−223

efficiency. Theoretical considerations, including DFT calculations, and experimental details are discussed that suggest the viability of a decamethylcobaltocene-mediated PCET pathway in this system; by extension we suggest that metallocene-mediated (e.g., Cp^*_2Cr) PCET pathways may be operative in previously studied Mo and Fe N_2-fixing systems that use metallocene reductants.[10−13,20]

$$BDE_{effective} = 1.37(pK_a) + 23.06(E^0) + C_H \quad (1)$$

Various observations of P_3^BFe complexes in the presence of acids and reductants suggested that this system might be capable of N_2-to-NH_3 conversion with lower driving force than that originally reported. Accordingly, we had observed that the treatment of $P_3^BFeN_2^-$ with KC_8 and weaker acids ($pK_a > 0$) led to greater than stoichiometric NH_3 formation (e.g., under unoptimized conditions [2,6-dimethylanilinium][OTf] afforded 2.1 equiv of NH_3 per Fe).[22] Similarly, the treatment of $P_3^BFeN_2^-$ with $[H(OEt_2)_2][BAr^F_4]$ ($HBAr^F_4$, BAr^F_4 = tetrakis-(3,5-bis(trifluoromethyl)phenyl)borate) and weaker reductants led to modest yields of NH_3. For example, under unoptimized conditions we had observed that decamethylcobaltocene (Cp^*_2Co) and $HBAr^F_4$ afforded 0.6 equiv of NH_3 per Fe.[22,23] Most recently, an apparent catalytic response was observed during a cyclic voltammetry experiment at the $P_3^BFeN_2^{0/-}$ couple (−2.1 V vs $Fc^{+/0}$) upon addition of excess $HBAr^F_4$ under an N_2 atmosphere. Electrolytic NH_3 generation by $P_3^BFe^+$ was observed at −2.4 V vs $Fc^{+/0}$ in Et_2O,[23] and Na/Hg (−2.4 V vs $Fc^{+/0}$ in THF)[16] could instead be used for N_2-to-NH_3 conversion catalysis (albeit less selectively and with low turnover). Finally, mixing $P_3^BFe^+$ with Cp^*_2Co in Et_2O at −78 °C under N_2 generates some $P_3^BFeN_2^-$ as observed by X-band EPR and Mössbauer spectroscopy (see the Supporting Information), suggesting that Cp^*_2Co is in principle a sufficiently strong reductant to trigger catalysis by $P_3^BFe^+$.

Treatment of $P_3^BFe^+$ with Cp^*_2Co and $[Ph_2NH_2][OTf]$, $[Ph_2NH_2][BAr^F_4]$, or $[PhNH_3][OTf]$ in Et_2O at −78 °C under an N_2 atmosphere affords catalytic yields of NH_3 (Table 1). Notably, the highest selectivity for NH_3 obtained among this series (72% at standard substrate loading; entry 1) is significantly improved compared to all previously described (molecular) Fe catalysts for N_2-to-NH_3 conversion.[20,24] Tripling the initial substrate loading (entry 2) nearly triples the NH_3 production with only modest loss in efficiency for NH_3 (63%). Preliminary attempts to further increase the initial substrate loading led to substantially decreased efficiency (entry 3). However, substrate reloading experiments (entries 4 and 5) maintained greater than 50% efficiency for NH_3 overall; a turnover number for NH_3 generation via two reloadings has been achieved as high as 89 in a single run (84 ± 8; entry 5). This is a high turnover number for a molecular Fe N_2-to-NH_3 conversion catalyst under any conditions.[20,25]

Table 1. N_2-to-NH_3 Conversion with P_3^EM Complexes (M = Fe, Co)[a]

	catalyst	Cp^*_2Co (equiv)	acid (equiv)	equiv of NH_3/Fe	% yield of NH_3/e^-
1	$P_3^BFe^+$	54	108[c]	12.8 ± 0.5	72 ± 3
2	$P_3^BFe^+$	162	322[c]	34 ± 1	63 ± 2
3	$P_3^BFe^+$	322	638[c]	26.7 ± 0.9	25 ± 1
4[b]	$P_3^BFe^+$	[162] × 2	[322] × 2[c]	56 ± 9	52 ± 9
5[b]	$P_3^BFe^+$	[162] × 3	[322] × 3[c]	84 ± 8	52 ± 5
6	$P_3^BFe^+$	54	108[d]	8 ± 1	42 ± 6
7	$P_3^BFe^+$	54	108[e]	7 ± 1	38 ± 7
8	$P_3^BFe^+$	162	322[e]	16 ± 3	29 ± 4
9	$P_3^{Si}FeN_2$	54	108[c]	1.2 ± 0.1	6 ± 1
10	$P_3^BCoN_2^-$	54	108[c]	1.1 ± 0.4	6 ± 2
11	$P_3^{Si}CoN_2$	54	108[c]	0 ± 0	0 ± 0

[a]The catalyst, acid, Cp^*_2Co, and Et_2O were sealed in a vessel at −196 °C under an N_2 atmosphere followed by warming to −78 °C and stirring. Yields are reported as an average of at least 2 runs; for individual experiments see the Supporting Information. [b]For these experiments the reaction was allowed to proceed for 3 h at −78 °C before cooling to −196 °C and furnishing with additional substrate and solvent. [c]$[Ph_2NH_2][OTf]$. [d]$[Ph_2NH_2][BAr^F_4]$. [e]$[PhNH_3][OTf]$.

The use of the more soluble acid $[Ph_2NH_2][BAr^F_4]$ (entry 6) provides significantly lower, but still catalytic, yields of NH_3. This more soluble acid presumably increases background reactivity with Cp^*_2Co (see the Supporting Information). Perhaps more significantly, $[PhNH_3][OTf]$ is a considerably weaker acid than $[Ph_2NH_2][OTf]$ (Figure 1), but still provides substantial catalytic yields of NH_3 (entries 7 and 8) and at efficiencies that compare well with those obtained previously using $HBAr^F_4$ and KC_8 despite a difference in driving force of nearly 100 kcal/mol.[23]

We also screened several related phosphine-ligated Fe−N_2 and Co−N_2 complexes[26,27] under the new standard reaction conditions with $[Ph_2NH_2][OTf]$ and Cp^*_2Co (entries 9−11) but found that none of these other systems were competent catalysts. While we anticipate that other catalyst systems for N_2-to-NH_3 conversion may yet be found that function under the conditions described herein,[20] certain features of the P_3^BFe system correlate with unusually productive catalysis.[27]

Also significant is that when $P_3^BFe^+$ is loaded with 322 equiv of $[Ph_2NH_2][OTf]$ and 162 equiv of Cp^*_2Co in Et_2O at −78 °C, very modest levels of N_2H_4 are detected (<1 equiv per Fe; see the Supporting Information).[9,20] We had previously reported that catalytic N_2 reduction with KC_8 and $HBAr^F_4$ yielded no detectable hydrazine, but observed that if hydrazine was added at the outset of a catalytic run, it was consumed.[6] When 5 equiv of N_2H_4 were added at the beginning of a catalytic run (again with 322 equiv of $[Ph_2NH_2][OTf]$ and 162 equiv of Cp^*_2Co), only 0.22 equiv of N_2H_4 (4.4% recovery) remained after workup. This result indicates that liberated hydrazine can also be reduced or disproportionated under the present conditions. That N_2H_4 is detected to any extent in the absence of initially added N_2H_4 under these conditions indicates that a late N−N cleavage mechanism to produce NH_3 (e.g., alternating or hybrid crossover) is accessible.[4,28] A recent report by Ashley and co-workers describes a phosphine-supported Fe system for which catalytic hydrazine formation is kinetically dominant.[20] Whether such a pathway is kinetically dominant in this system is as yet unclear.[23,29]

The P_3^BFe speciation under turnover conditions was probed via freeze-quench Mössbauer spectroscopy.[23] The Mössbauer spectrum of a catalytic reaction mixture after 5 min of reaction time (Figure 2) reveals the presence of multiple species featuring well-resolved sets of quadrupole doublets. The spectrum is satisfactorily simulated with $P_3^BFeN_2$ (δ = 0.55 mm/s, ΔE_Q = 3.24 mm/s, 32%; Figure 2, green), $P_3^BFeN_2^-$ (δ = 0.40 mm/s, ΔE_Q = 0.98 mm/s, 26%; Figure 2, blue),[23,30] an unknown, likely P_3^B metalated Fe species (δ = 0.42 mm/s, ΔE_Q = 1.84 mm/s, 18%; Figure 2, yellow), and a final species that is modeled with δ = 0.96 mm/s and ΔE_Q = 3.10 mm/s (24%; Figure 2, orange). The broad nature of this last signal and its overlap with other features in the spectrum prevents its precise

DOI: 10.1021/acscentsci.7b00014
ACS Cent. Sci. 2017, 3, 217−223

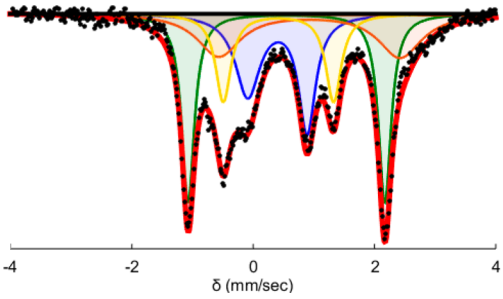

Figure 2. Mössbauer spectrum at 80 K with 50 mT applied parallel field of a freeze-quenched catalytic reaction (54 equiv of Cp^*_2Co, 108 equiv of $[Ph_2NH_2][OTf]$, 1 equiv of $P_3^B[^{57}Fe]^+$) after 5 min of reaction time.

assignment, but its high isomer shift and large quadrupole splitting are suggestive of a tetrahedral, S = 2 Fe(II) complex.[31,32] The Mössbauer spectrum of a catalytic reaction mixture after 30 min was also analyzed (see the Supporting Information). The spectrum still shows $P_3^BFeN_2$ (53%), the same unknown P_3^BFe species (18%), and again a tetrahedral, high-spin Fe(II) component (22%). However, $P_3^BFe^+$ is now present (δ = 0.75 mm/s, ΔE_Q = 2.55 mm/s, 8%) and $P_3^BFeN_2^-$ is no longer observed. The reloading experiments described above provide strong evidence that "P_3^BFe" species represent an "active catalyst" population; interpretation of the relative speciation via spectroscopy should hence bear on the mechanism of the overall catalysis.

The appearance of a presumed high-spin (S = 2), tetrahedral Fe(II) species during catalysis (ca. 25%) might arise via dechelation of a phosphine arm. This species could represent an off-path state or a downstream deactivation product. Interestingly, under the present catalytic conditions we do not observe the borohydrido−hydrido species $P_3^B(\mu\text{-H})Fe(H)(L)$ (L = N_2 or H_2); this species was postulated to be an off-path state during N_2-to-NH_3 conversion catalysis using $HBAr^F_4$ and KC_8 and was the major component observed at early times (ca. 60% at 5 min).[23] It therefore appears that a larger fraction of the "P_3^BFe" species are in a catalytically on-path state at early reaction times under these new catalytic conditions.

Additionally, the presence of a significant degree of $P_3^BFeN_2^-$ (Figure 2) at an early time point is distinct from conditions with $HBAr^F_4$ and KC_8.[23] This observation is consistent with the notion that protonation of $P_3^BFeN_2^-$ is slowed under the present conditions, likely as a result of the insolubility of the triflate salt $[Ph_2NH_2][OTf]$ and its attenuated acidity relative to $HBAr^F_4$.[17,18,33] Clearly, differences in the rates of key elementary steps under the new conditions described here may lead to new mechanistic scenarios for N_2-to-NH_3 conversion.

The improved catalytic efficiency at significantly lower driving force warrants additional consideration. When using $HBAr^F_4$ and KC_8 we have previously suggested that protonation of $P_3^BFeN_2^-$, which itself can be generated by reduction of $P_3^BFeN_2$, to produce $P_3^BFe{-}N{=}NH$ is a critical first step; $P_3^BFe{-}N{=}NH$ can then be trapped by acid to produce spectroscopically observable $P_3^BFe{=}N{-}NH_2^+$.[29] These steps, shown in eqs 2a and 2b, represent an ET−PT pathway. A PT−ET pathway, where $P_3^BFeN_2$ is sufficiently basic to be protonated to generate $P_3^BFe{-}N{=}NH^+$ as a first step, followed by ET, is also worth considering (eqs 3a and 3b). A direct PCET pathway (eq 4), where H atom delivery to $P_3^BFeN_2$ occurs, thus obviating the need to access either $P_3^BFeN_2^-$ or $P_3^BFe{-}N{=}NH^+$, needs also to be considered.

$$P_3^BFeN_2 + e^- \rightarrow P_3^BFeN_2^- \quad (2a)$$

$$P_3^BFeN_2^- + H^+ \rightarrow P_3^BFe{-}N{=}NH \quad (2b)$$

$$P_3^BFeN_2 + H^+ \rightarrow P_3^BFe{-}N{=}NH^+ \quad (3a)$$

$$P_3^BFe{-}N{=}NH^+ + e^- \rightarrow P_3^BFe{-}N{=}NH \quad (3b)$$

$$P_3^BFeN_2 + H\bullet \rightarrow P_3^BFe{-}N{=}NH \quad (4)$$

Initial PT to $P_3^BFeN_2$ to generate $P_3^BFe{-}N{=}NH^+$ (eq 3a) is unlikely under the present conditions due to the high predicted acidity of $P_3^BFe{-}N{=}NH^+$ (pK_a = −3.7; estimated via DFT; see the Supporting Information); efficient generation of such a species seems implausible for acids whose pK_a's are calculated at 1.4 ($Ph_2NH_2^+$) and 6.8 ($PhNH_3^+$) in Et_2O (Table 2). We note that $[Ph_2NH_2][OTf]$ does not react productively with $P_3^BFeN_2$ at −78 °C in Et_2O, as analyzed by Mössbauer spectroscopy.

Table 2. Calculated pK_a Values and BDEs of Selected Species[a]

species	pK_a	BDE[b]
$Ph_2NH_2^+$	1.4[c]	
$PhNH_3^+$	6.8	
lutidinium	14.5	
endo-$Cp^*Co(\eta^4\text{-}C_5Me_5H)^+$	16.8	31
exo-$Cp^*Co(\eta^4\text{-}C_5Me_5H)^+$	16.8	31
endo-$Cp^*Cr(\eta^4\text{-}C_5Me_5H)^+$	17.3	37
exo-$Cp^*Cr(\eta^4\text{-}C_5Me_5H)^+$	12.1	30
$P_3^BFe{-}N{=}NH^+$	−3.7	
$P_3^BFe{-}N{=}NH$	38.7	35
$P_3^BFe{=}N{-}NH_2^+$	14.4	51
$P_3^BFe{=}N{-}NH_2$		47
$[HIPTN_3N]Mo{-}N{=}NH$		51

[a]Calculations were performed using the M06-L[34] functional with a def2-TZVP basis set on Fe and Mo and a def2-SVP basis set on all other atoms[35] (see the Supporting Information). [b]In kcal/mol. [c]pK_a values were calculated in Et_2O and reported relative to $(Et_2O)_2H^+$.

Focusing instead on the PCET pathway (eq 4), the DFT-calculated BDE_{N-H} for $P_3^BFe{-}N{=}NH$ (35 kcal/mol; Table 2; see the Supporting Information for details)[36] is larger than the effective BDE[21] of either $Cp^*_2Co/Ph_2NH_2^+$ or $Cp^*_2Co/PhNH_3^+$ (25 and 31 kcal/mol, respectively). This suggests that PCET (eq 4) is plausible on thermodynamic grounds. Given that we have employed Cp^*_2Co in this study, and that this and also Cp_2Co and Cp^*_2Cr have been effective in other N_2-fixing molecular catalyst systems,[10−13,20] we have explored via DFT several putative metallocene-derived PCET reagents. Independent studies of H_2 evolution from cobaltocene have invoked a protonated cobaltocene intermediate.[37−39] The observation of a background H_2 evolution reaction (HER) when employing metallocene reductants, but in the absence of an N_2-to-NH_3 conversion catalyst, suggests that metallocene protonation is kinetically competent.[13,40] Based on the analysis we describe below, we propose that protonated metallocenes may serve as discrete and highly active H• sources for PCET.

We find that the formation of *endo*- and *exo*-$Cp^*Co(\eta^4\text{-}C_5Me_5H)^+$ is predicted to be thermodynamically favorable via

DOI: 10.1021/acscentsci.7b00014
ACS Cent. Sci. 2017, 3, 217−223

protonation of Cp^*_2Co by either $Ph_2NH_2^+$ or $PhNH_3^+$ (−21 and −13 kcal/mol, respectively; Figure 3A).[41,42] We have

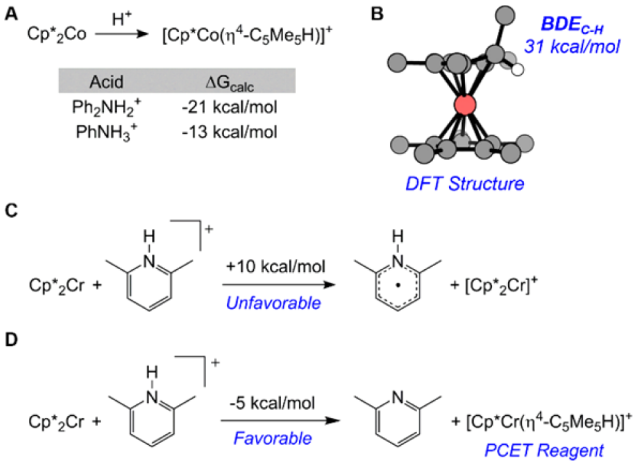

Figure 3. (A) Calculated free-energy changes for the protonation of Cp^*_2Co. (B) DFT optimized structure of *endo*-$Cp^*Co(\eta^4\text{-}C_5Me_5H)^+$ (methyl protons omitted for clarity). (C) The unfavorable reduction of 2,6-lutidinium by Cp^*_2Cr with the calculated free energy change. (D) The favorable protonation of Cp^*_2Cr by lutidinium with the calculated free energy change.

calculated the BDE_{C-H}'s for both *endo*- and *exo*-$Cp^*Co(\eta^4\text{-}C_5Me_5H)^+$ as 31 kcal/mol (Figure 3B; Table 2), indicating that they should be among the strongest PCET reagents accessible in this catalyst cocktail. Indeed, they would be among the strongest PCET reagents known.[21]

We anticipate that these species would be extremely unstable in solution and hence difficult to detect in situ, but via trapping in the solid state by rapid precipitation from toluene we have isolated a species whose EPR data and chemical behavior are consistent with $\{Cp^*Co(\eta^4\text{-}C_5Me_5H)\}\{OTf\}$. Accordingly, slow addition of a toluene solution of Cp^*_2Co at −78 °C to triflic acid (HOTf) leads to the instantaneous precipitation of a purple solid that can be handled only at low temperature. The purple solid is characterized at 77 K by powder EPR spectroscopy via its highly structured signal. By contrast, at this temperature $S = 1/2$ Cp^*_2Co does not display a discernible EPR signal (see the Supporting Information). The new signal shows strong Co hyperfine coupling and significant *g*-anisotropy, consistent with a new $S = 1/2$ cobalt species (Figure 4). Furthermore, the resulting EPR signal is slightly perturbed when this purple solid is instead generated from the reaction between deuterated triflic acid (DOTf) and Cp^*_2Co (see the Supporting Information), suggesting that the acidic proton is directly associated with the new Co species and consistent with its assignment as a protonated decamethylcobaltocene species. Close inspection of these spectra indicates that they likely represent a mixture of two signals arising from similar Co-containing complexes. This observation is consistent with the presence of both *endo*- and *exo*-$Cp^*Co(\eta^4\text{-}C_5Me_5H)^+$, as is to be expected given that they are predicted to be nearly isoenergetic. Allowing the purple precipitate to warm to room temperature either as a solid or as a stirred suspension in toluene leads to the formation of H_2 and $Cp^*_2Co^+$ (see the Supporting Information).

To better understand the potential role of PCET in N_2-to-NH_3 conversion catalysis by P_3^BFe, we have additionally calculated the N−H bond strengths (Table 2) of several early

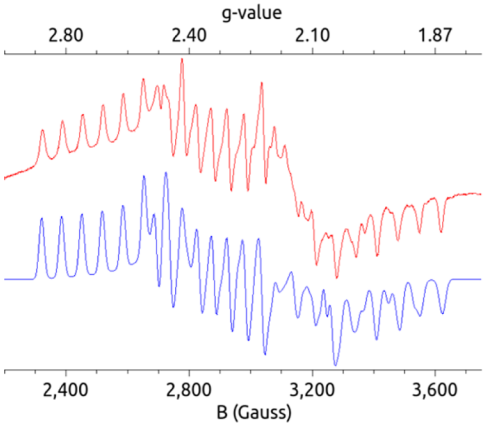

Figure 4. X-band 77 K powder EPR spectrum (red) and simulation (blue) of the isolated purple precipitate (assigned as *endo*- and *exo*-$Cp^*Co(\eta^4\text{-}C_5Me_5H)^+$) from reaction between Cp^*_2Co and HOTf at −78 °C (see the Supporting Information for simulation parameters).

stage candidate intermediates, including the aforementioned $P_3^BFe{-}N{=}NH$ (35 kcal/mol), $P_3^BFe{=}N{-}NH_2^+$ (51 kcal/mol), and $P_3^BFe{=}N{-}NH_2$ (47 kcal/mol). We conclude that PCET from $Cp^*Co(\eta^4\text{-}C_5Me_5H)^+$ to generate intermediates of these types is thermodynamically favorable in each case.[43] To generate the first and most challenging intermediate (eq 5), the enthalpic driving force for PCET is estimated at ∼4 kcal/mol (ΔG_{calc} = −9 kcal/mol). This driving force and, hence, the plausibility of PCET steps, increase sharply as further downstream $Fe{-}N_xH_y$ intermediates are considered.[44−47]

$$P_3^BFeN_2 + Cp^*Co(\eta^4\text{-}C_5Me_5H)^+ \rightarrow P_3^BFe{-}N{=}NH + Cp^*_2Co^+ \quad (5)$$

Given the prevalence of metallocene reductants in N_2-to-NH_3 (or -N_2H_4) conversion,[10−13,20] especially for the well-studied Mo catalyst systems, it is worth considering metallocene-mediated PCET more generally. For instance, a role for ET/PT steps (or conversely PT/ET) in N_2-to-NH_3 conversion catalyzed by $[HIPTN_3N]Mo$ ($HIPTN_3N$ = $[(3,5\text{-}(2,4,6\text{-}{}^iPr_3C_6H_2)_2C_6H_3NCH_2CH_2)_3N]^{3-}$, a bulky triamidoamine ligand) has been frequently posited.[48−52] But PCET steps may play a critical role, too. In the latter context, we note reports from Schrock and co-workers that have shown that both acid and reductant are required to observe productive reactivity with $[HIPTN_3N]MoN_2$. These observations are consistent with PCET to generate $[HIPTN_3N]Mo{-}N{=}NH$.[52] A PCET scenario has been discussed in the general context of N_2-to-NH_3 conversion, where a lutidinyl radical intermediate formed via ET from Cp^*_2Cr was suggested as a PCET reagent that can be generated in situ.[40,53] However, our own calculations predict that the lutidinyl radical should not be accessible with Cp^*_2Cr as the reductant (ΔG_{calc} = +10 kcal/mol; Figure 3C).[54−56] We instead propose protonation of Cp^*_2Cr by the lutidinium acid as more plausible (ΔG_{calc} = −5.3 kcal/mol; Figure 3D) to generate a highly reactive decamethylchromocene-derived PCET reagent.

While N−H bond strengths have not been experimentally determined for the $[HIPTN_3N]Mo$ system, using available published data we deduce the N−H bond of $[HIPTN_3N]Mo{-}N{=}NH$ to be ca. 49 kcal/mol and we calculate it via DFT (truncated $HIPTN_3N$; see the Supporting Information) as 51 kcal/mol.[57] The BDE_{N-H} for this Mo diazenido species is

DOI: 10.1021/acscentsci.7b00014
ACS Cent. Sci. 2017, 3, 217−223

hence much larger than we predict for $P_3^BFe{-}N{=}NH$ (35 kcal/mol), perhaps accounting for its higher stability.[S2] A PCET reaction between *endo*-Cp*Cr(η^4-C_5Me_5H)$^+$ (BDE_{calc} = 37 kcal/mol) and [HIPTN$_3$N]MoN_2 to generate [HIPTN$_3$N]-Mo−N=NH and $Cp^*_2Cr^+$ would be highly exergonic. Furthermore, we predict a similarly weak BDE_{C-H} for Cp-protonated cobaltocene, CpCo(η^4-C_5H_6)$^+$ (BDE_{calc} = 35 kcal/mol). These considerations are consistent with the reported rapid formation of [HIPTN$_3$N]Mo−N=NH using either Cp^*_2Cr or Cp_2Co in the presence of lutidinium acid.[S8]

To close, we have demonstrated catalytic N_2-to-NH_3 conversion by $P_3^BFe^+$ at a much lower driving force (nearly 100 kcal/mol) than originally reported via combination of a weaker reductant (Cp^*_2Co) and acid ([Ph_2NH_2][OTf] or [$PhNH_3$][OTf]). Significantly improved efficiency for NH_3 formation is observed (up to 72% at standard substrate loading), and by reloading additional substrate at low temperature a turnover number that is comparatively high for a synthetic molecular Fe catalyst (84 ± 8 equiv of NH_3 per Fe) has been achieved. Freeze-quench Mössbauer spectroscopy under turnover conditions reveals differences in the speciation of P_3^BFe compared to previous studies with $HBAr^F_4$ and KC_8, suggesting changes in the rates of key elementary steps. Using DFT calculations we have considered the viability of a decamethylcobaltocene-mediated PCET pathway as an additional contributor to the previously formulated ET−PT and PT−ET pathways. Based on our calculations, we propose that protonated metallocenes should serve as discrete, very reactive PCET reagents in N_2-to-NH_3 conversion catalysis. Furthermore, we present preliminary experimental data that suggests that protonated decamethylcobaltocene can be accessed synthetically and that such a species may be a potent PCET reagent. Indeed, the achievement of high efficiency for N_2-to-NH_3 conversion by both P_3^BFe and various Mo catalysts that benefit from metallocene reductants raises the intriguing possibility that metallocene-based PCET reactivity is a potentially widespread and overlooked mechanism. Efforts are underway to experimentally probe such pathways.

■ ASSOCIATED CONTENT

Supporting Information

The Supporting Information is available free of charge on the ACS Publications website at DOI: 10.1021/acscentsci.7b00014.

Experimental procedures, spectroscopic details, and computational methods (PDF)

Collection of 48 models (MOL)

■ AUTHOR INFORMATION

Corresponding Author

*E-mail: jpeters@caltech.edu.

ORCID

Jonas C. Peters: 0000-0002-6610-4414

Author Contributions

†M.J.C., T.J.D.C., and B.D.M. contributed equally to this work.

Notes

The authors declare no competing financial interest.

■ ACKNOWLEDGMENTS

This work was supported by the NIH (GM 070757) and the Gordon and Betty Moore Foundation. This work used the Extreme Science and Engineering Discovery Environment (XSEDE), which is supported by National Science Foundation Grant No. ACI-1053575. M.J.C., T.J.D.C., and B.D.M. acknowledge the support of the NSF for Graduate Fellowships (GRFP).

■ REFERENCES

(1) Smil, V. *Enriching the Earth*: MIT Press: Cambridge, 2001.

(2) van der Ham, C. J. M.; Koper, M. T. M.; Hetterscheid, D. G. H. Challenges in Reduction of Dinitrogen by Proton and Electron Transfer. *Chem. Soc. Rev.* **2014**, *43*, 5183−5191.

(3) Shaver, M. P.; Fryzuk, M. D. Activation of Molecular Nitrogen: Coordination, Cleavage and Functionalization of N_2 Mediated By Metal Complexes. *Adv. Synth. Catal.* **2003**, *345*, 1061−1076.

(4) MacLeod, K. C.; Holland, P. L. Recent Developments in the Homogeneous Reduction of Dinitrogen by Molybdenum and Iron. *Nat. Chem.* **2013**, *5*, 559−565.

(5) Hoffman, B. M.; Lukoyanov, D.; Yang, Z.-Y.; Dean, D. R.; Seefeldt, L. C. Mechanism of Nitrogen Fixation by Nitrogenase: The Next Stage. *Chem. Rev.* **2014**, *114*, 4041−4062.

(6) Anderson, J. S.; Rittle, J.; Peters, J. C. Catalytic Conversion of Nitrogen to Ammonia by an Iron Model Complex. *Nature* **2013**, *501*, 84−87.

(7) Creutz, S. E.; Peters, J. C. Catalytic Reduction of N_2 to NH_3 by an Fe−N_2 Complex Featuring a C-Atom Anchor. *J. Am. Chem. Soc.* **2014**, *136*, 1105−1115.

(8) Ung, G.; Peters, J. C. Low-Temperature N_2 Binding to Two-Coordinate L_2Fe^0 Enables Reductive Trapping of $L_2FeN_2^-$ and NH_3 Generation. *Angew. Chem., Int. Ed.* **2015**, *54*, 532−535.

(9) Kuriyama, S.; Arashiba, K.; Nakajima, K.; Matsuo, Y.; Tanaka, H.; Ishii, K.; Yoshizawa, K.; Nishibayashi, Y. Catalytic Transformation of Dinitrogen into Ammonia and Hydrazine by Iron-Dinitrogen Complexes Bearing Pincer Ligand. *Nat. Commun.* **2016**, *7*, 12181.

(10) Yandulov, D. V.; Schrock, R. R. Catalytic Reduction of Dinitrogen to Ammonia at a Single Molybdenum Center. *Science* **2003**, *301*, 76−78.

(11) Arashiba, K.; Miyake, Y.; Nishibayashi, Y. A Molybdenum Complex Bearing PNP-Type Pincer Ligands Leads to the Catalytic Reduction of Dinitrogen into Ammonia. *Nat. Chem.* **2011**, *3*, 120−125.

(12) Kuriyama, S.; Arashiba, K.; Nakajima, K.; Tanaka, H.; Kamaru, N.; Yoshizawa, K.; Nishibayashi, Y. Catalytic Formation of Ammonia from Molecular Dinitrogen by Use of Dinitrogen-Bridged Dimolybdenum−Dinitrogen Complexes Bearing PNP-Pincer Ligands: Remarkable Effect of Substituent at PNP-Pincer Ligand. *J. Am. Chem. Soc.* **2014**, *136*, 9719−9731.

(13) Arashiba, K.; Kinoshita, E.; Kuriyama, S.; Eizawa, A.; Nakajima, K.; Tanaka, H.; Yoshizawa, K.; Nishibayashi, Y. Catalytic Reduction of Dinitrogen to Ammonia by Use of Molybdenum−Nitride Complexes Bearing a Tridentate Triphosphine as Catalysts. *J. Am. Chem. Soc.* **2015**, *137*, 5666−5669.

(14) The enthalpic driving force ($\Delta\Delta H_f$) has been estimated here by taking $3(BDE_{H\bullet} - BDE_{effective})$, where BDE is bond dissociation enthalpy. This allows for an evaluation of the driving force for a given reaction with respect to that for a hypothetical N_2-to-NH_3 conversion catalyst that uses H_2 as the proton and electron source. This is achieved by using Bordwell's equation (with the assumption that $S(X\bullet) = S(XH)$; see the Supporting Information) and literature values (see refs 15−19 and 21) for pK_a, redox potential, the enthalpy of reaction for $H^+ + e^- \rightarrow H\bullet$ (C_H = 66 kcal/mol in THF), and the energy of H• in THF (52 kcal/mol).

(15) Bordwell, F. G.; Cheng, J. P.; Harrelson, J. A. Homolytic Bond Dissociation Energies in Solution from Equilibrium Acidity and Electrochemical Data. *J. Am. Chem. Soc.* **1988**, *110*, 1229−1231.

(16) Connelly, N. G.; Geiger, W. E. Chemical Redox Agents for Organometallic Chemistry. *Chem. Rev.* **1996**, *96*, 877−910.

(17) Garrido, G.; Rosés, M.; Ràfols, C.; Bosch, E. Acidity of Several Anilinium Derivatives in Pure Tetrahydrofuran. *J. Solution Chem.* **2008**, *37*, 689−700.

(18) Kaljurand, I.; Kütt, A.; Sooväli, L.; Rodima, T.; Mäemets, V.; Leito, I.; Koppel, I. A. Extension of the Self-Consistent Spectrophotometric Basicity Scale in Acetonitrile to a Full Span of 28 pKa Units: Unification of Different Basicity Scales. *J. Org. Chem.* **2005**, *70*, 1019−1028.
(19) Cappellani, E. P.; Drouin, S. D.; Jia, G.; Maltby, P. A.; Morris, R. H.; Schweitzer, C. T. Effect of the Ligand and Metal on the pK_a Values of the Dihydrogen Ligand in the Series of Complexes $[M(H_2)H(L)_2]^+$, M = Fe, Ru, Os, Containing Isosteric Ditertiaryphosphine Ligands, L. *J. Am. Chem. Soc.* **1994**, *116*, 3375−3388.
(20) While initiating our studies we became aware of a phosphine-supported Fe system that catalyzes N_2-to-N_2H_4 conversion using Cp^*_2Co and $[Ph_2NH_2][OTf]$ with efficiency as high as 72% for e^- delivery to N_2: Hill, P. J.; Doyle, L. R.; Crawford, A. D.; Myers, W. K.; Ashley, A. E. Selective Catalytic Reduction of N_2 to N_2H_4 by a Simple Fe Complex. *J. Am. Chem. Soc.* **2016**, *138*, 13521−13524.
(21) Warren, J. J.; Tronic, T. A.; Mayer, J. M. Thermochemistry of Proton-Coupled Electron Transfer Reagents and its Implications. *Chem. Rev.* **2010**, *110*, 6961−7001.
(22) Anderson, J. S. *Catalytic conversion of nitrogen to ammonia by an iron model complex*; Ph.D. Thesis, California Institute of Technology: September 2013.
(23) Del Castillo, T. J.; Thompson, N. B.; Peters, J. C. A Synthetic Single-Site Fe Nitrogenase: High Turnover, Freeze-Quench ^{57}Fe Mössbauer Data, and a Hydride Resting State. *J. Am. Chem. Soc.* **2016**, *138*, 5341−5350.
(24) Previously reported molecular Fe catalysts for N_2-to-NH_3 conversion utilize KC_8 and $HBAr^F_4$ and achieve NH_3 selectivities ≤45% with respect to their limiting reagent (see refs 6−9) at a similar reductant loading. Lower selectivities are observed with higher loading (see refs 6 and 23).
(25) In catalytic runs performed with labeled $[Ph_2{}^{15}NH_2][OTf]$ under an atmosphere of natural abundance $^{14}N_2$ the production of exclusively $^{14}NH_3$ is observed, demonstrating that the NH_3 formed during catalysis is derived from N_2 and not degradation of the acid (see the Supporting Information).
(26) Whited, M. T.; Mankad, N. P.; Lee, Y.; Oblad, P. F.; Peters, J. C. Dinitrogen Complexes Supported by Tris(phosphino)silyl Ligands. *Inorg. Chem.* **2009**, *48*, 2507−2517.
(27) Del Castillo, T. J.; Thompson, N. B.; Suess, D. L. M.; Ung, G.; Peters, J. C. Evaluating Molecular Cobalt Complexes for the Conversion of N_2 to NH_3. *Inorg. Chem.* **2015**, *54*, 9256−9262.
(28) Rittle, J.; Peters, J. C. An Fe-N_2 Complex That Generates Hydrazine and Ammonia via Fe=NNH_2: Demonstrating a Hybrid Distal-to-Alternating Pathway for N_2 Reduction. *J. Am. Chem. Soc.* **2016**, *138*, 4243−4248.
(29) Anderson, J. S.; Cutsail, G. E.; Rittle, J.; Connor, B. A.; Gunderson, W. A.; Zhang, L.; Hoffman, B. M.; Peters, J. C. Characterization of an Fe≡N−NH_2 Intermediate Relevant to Catalytic N_2 Reduction to NH_3. *J. Am. Chem. Soc.* **2015**, *137*, 7803−7809.
(30) The presence of $P_3{}^BFeN_2{}^-$ was confirmed by freeze-quench EPR spectroscopy experiments (see the Supporting Information). The asymmetry observed in the Mössbauer lineshapes is characteristic of this species. A redox equilibrium between $P_3{}^BFeN_2{}^{0/-}$ and $Cp^*_2Co^{+/0}$ is also observed in the reaction of $P_3{}^BFe^+$ with excess Cp^*_2Co in the absence of acid (see the Supporting Information).
(31) The distinct properties of tetrahedral, high spin Fe(II) lead to high isomer shifts (0.9−1.3) and large quadrupole splittings (>2.5) that are characteristic of these types of species: Münck, E. In *Physical Methods in Bioinorganic Chemistry: Spectroscopy and Magnetism*; Que, L., Jr., Ed.; University Science Books: Sausalito, CA, 2000; pp 287−320.
(32) Daifuku, S. L.; Kneebone, J. L.; Snyder, B. E. R.; Neidig, M. L. Iron(II) Active Species in Iron−Bisphosphine Catalyzed Kumada and Suzuki−Miyaura Cross-Couplings of Phenyl Nucleophiles and Secondary Alkyl Halides. *J. Am. Chem. Soc.* **2015**, *137*, 11432−11444.
(33) Hamashima, Y.; Somei, H.; Shimura, Y.; Tamura, T.; Sodeoka, M. Amine-Salt-Controlled, Catalytic Asymmetric Conjugate Addition of Various Amines and Asymmetric Protonation. *Org. Lett.* **2004**, *6*, 1861−1864.
(34) Zhao, Y.; Truhlar, D. G. A New Local Density Functional for Main-Group Thermochemistry, Transition Metal Bonding, Thermochemical Kinetics, and Noncovalent Interactions. *J. Chem. Phys.* **2006**, *125*, 194101.
(35) Weigend, F.; Ahlrichs, R. Balanced Basis Sets of Split Valence, Triple Zeta Valence and Quadruple Zeta Valence Quality for H to Rn: Design and Assessment of Accuracy. *Phys. Chem. Chem. Phys.* **2005**, *7*, 3297−3305.
(36) Experimental $BDE_{N\text{-}H}$'s for related species ($P_3{}^{Si}Fe-C{=}NH^+$, $P_3{}^{Si}Fe-C{=}NH$, $P_3{}^{Si}Fe-C{=}N(Me)H^+$, $P_3{}^{Si}Fe-C{=}N(Me)H$, and $P_3{}^{Si}Fe-N{=}N(Me)H^+$) have been measured and are in good agreement with the BDE_{N-H} values calculated using the DFT methods described in this work (see the Supporting Information for full details): Rittle, J.; Peters, J. C. N−H Bond Dissociation Enthalpies and Facile H Atom Transfers for Early Intermediates of Fe−N_2 and Fe−CN Reductions. *J. Am. Chem. Soc.* **2017**, in press, DOI: 10.1021/jacs.6b12861.
(37) Koelle, U.; Infelta, P. P.; Graetzel, M. Kinetics and Mechanism of the Reduction of Protons to Hydrogen by Cobaltocene. *Inorg. Chem.* **1988**, *27*, 879−883.
(38) Pitman, C. L.; Finster, O. N. L.; Miller, A. J. M. Cyclopentadiene-Mediated Hydride Transfer from Rhodium Complexes. *Chem. Commun.* **2016**, *52*, 9105−9108.
(39) Quintana, L. M. A.; Johnson, S. I.; Corona, S. L.; Villatoro, W.; Goddard, W. A.; Takase, M. K.; VanderVelde, D. G.; Winkler, J. R.; Gray, H. B.; Blakemore, J. D. Proton−hydride Tautomerism in Hydrogen Evolution Catalysis. *Proc. Natl. Acad. Sci. U. S. A.* **2016**, *113*, 6409−6414.
(40) Munisamy, T.; Schrock, R. R. An Electrochemical Investigation of Intermediates and Processes Involved in the Catalytic Reduction of Dinitrogen by [HIPTN$_3$N]Mo (HIPTN$_3$N = (3,5-(2,4,6-I-Pr$_3$C$_6$H$_2$)$_2$C$_6$H$_3$NCH$_2$CH$_2$)$_3$N). *Dalton Trans.* **2012**, *41*, 130−137.
(41) Efforts to instead optimize a metal hydride species, $[Cp^*_2Co-H]^+$, led to hydride transfer to the ring system. Nevertheless, reactive transition metal hydride radical cations are also known to exhibit PCET behavior.
(42) Hu, Y.; Shaw, A. P.; Estes, D. P.; Norton, J. R. Transition-Metal Hydride Radical Cations. *Chem. Rev.* **2016**, *116*, 8427−8462.
(43) The dissolution equilibria and kinetics of the insoluble reagents used complicate analysis of the kinetics of individual ET, PT, and PCET steps. However, the low activation barriers ($G^‡$ < 9 kcal/mol) calculated for all proposed PCET reactions are consistent with these reactions being kinetically accessible (see the Supporting Information for full details).
(44) Studies (see refs 45−47) have shown that the Marcus cross-relation holds quite well for many PCET reactions. This is indicative of a substantial correlation between thermodynamic driving force and reaction kinetics; it is, however, unclear whether the proposed reactivity would demonstrate such behavior.
(45) Roth, J. P.; Yoder, J. C.; Won, T.-J.; Mayer, J. M. Application of the Marcus Cross Relation to Hydrogen Atom Transfer Reactions. *Science* **2001**, *294*, 2524−2526.
(46) Mayer, J. M.; Rhile, I. J. Thermodynamics and Kinetics of Proton-Coupled Electron Transfer: Stepwise vs. Concerted Pathways. *Biochim. Biophys. Acta, Bioenerg.* **2004**, *1655*, 51−58.
(47) Hammes-Schiffer, S. Theoretical Perspectives on Proton-Coupled Electron Transfer Reactions. *Acc. Chem. Res.* **2001**, *34*, 273−281.
(48) Studt, F.; Tuczek, F. Energetics and Mechanism of a Room-Temperature Catalytic Process for Ammonia Synthesis (Schrock Cycle): Comparison with Biological Nitrogen Fixation. *Angew. Chem., Int. Ed.* **2005**, *44*, 5639−5642.
(49) Reiher, M.; Le Guennic, B.; Kirchner, B. Theoretical Study of Catalytic Dinitrogen Reduction under Mild Conditions. *Inorg. Chem.* **2005**, *44*, 9640−9642.
(50) Studt, F.; Tuczek, F. Theoretical, Spectroscopic, and Mechanistic Studies on Transition-Metal Dinitrogen Complexes:

DOI: 10.1021/acscentsci.7b00014
ACS Cent. Sci. 2017, 3, 217−223

Implications to Reactivity and Relevance to the Nitrogenase Problem. *J. Comput. Chem.* **2006**, *27*, 1278−1291.
(51) Thimm, W.; Gradert, C.; Broda, H.; Wennmohs, F.; Neese, F.; Tuczek, F. Free Reaction Enthalpy Profile of the Schrock Cycle Derived from Density Functional Theory Calculations on the Full [MoHIPTN$_3$N] Catalyst. *Inorg. Chem.* **2015**, *54*, 9248−9255.
(52) Yandulov, D. V.; Schrock, R. R. Studies Relevant to Catalytic Reduction of Dinitrogen to Ammonia by Molybdenum Triamidoamine Complexes. *Inorg. Chem.* **2005**, *44*, 1103−1117.
(53) Pappas, I.; Chirik, P. J. Catalytic Proton Coupled Electron Transfer from Metal Hydrides to Titanocene Amides, Hydrazides and Imides: Determination of Thermodynamic Parameters Relevant to Nitrogen Fixation. *J. Am. Chem. Soc.* **2016**, *138*, 13379−13389.
(54) Although our calculations for a hypothetical lutidinyl radical predict a weak N−H bond (BDE$_{N-H}$ ∼ 35 kcal/mol), the oxidation potential of this species is calculated to be −1.89 V vs Fc$^{+/0}$ in THF (see the Supporting Information). Experimental determination of this reduction potential for calibration has been contentious; however, our calculated reduction potential is similar to that previously calculated for pyridinium in aqueous media (−1.37 V vs SCE; see refs 55 and 56).
(55) Yan, Y.; Zeitler, E. L.; Gu, J.; Hu, Y.; Bocarsly, A. B. Electrochemistry of Aqueous Pyridinium: Exploration of a Key Aspect of Electrocatalytic Reduction of CO_2 to Methanol. *J. Am. Chem. Soc.* **2013**, *135*, 14020−14023.
(56) Keith, J. A.; Carter, E. A. Theoretical Insights into Pyridinium-Based Photoelectrocatalytic Reduction of CO_2. *J. Am. Chem. Soc.* **2012**, *134*, 7580−7583.
(57) It has been reported that [HIPTN$_3$N]MoN$_2^-$/[HIPTN$_3$N]Mo−N═NH is in equilibrium with DBU/DBUH$^+$ (DBU = 1,8-diazabicyclo[5.4.0]undec-7-ene; pK_a = 18.5 in THF; see refs 17 and 18). Taken with the reported reduction potential of [HIPTN$_3$N]MoN$_2$ ($E_{1/2}$ = − 1.81 V vs Fc$^{+/0}$ in THF, see ref 52), the experimental BDE can be approximated with the Bordwell equation and the enthalpy of reaction for $H^+ + e^- \rightarrow H^\bullet$ (see refs 15 and 19).
(58) In addition to lutidinium salts, [Et$_3$NH][OTf] has been shown to affect the formation of [HIPTN$_3$N]Mo−N═NH from [HIPTN$_3$N]MoN$_2$ in the presence of metallocene reductants (see ref 52).

DOI: 10.1021/acscentsci.7b00014
ACS Cent. Sci. 2017, 3, 217−223